

## Microwave accelerated synthesis of isoxazole hydrazide inhibitors of the system $\text{Sx}_{\text{c}-}$ transporter: Initial homology model



Afnan A. Matti <sup>a,b</sup>, Joseph Mirzaei <sup>a,b</sup>, John Rudolph <sup>a</sup>, Stephen A. Smith <sup>a</sup>, Jayme L. Newell <sup>a</sup>, Sarjubhai A. Patel <sup>a</sup>, Michael R. Braden <sup>a</sup>, Richard J. Bridges <sup>a</sup>, Nicholas R. Natale <sup>a,b,\*</sup>

<sup>a</sup> Department of Biomedical & Pharmaceutical Sciences, Center for Structural & Functional Neuroscience, The University of Montana, Missoula, MT 59812, United States

<sup>b</sup> Medicinal Chemistry Graduate Program, The University of Montana, Missoula, MT 59812, United States

### ARTICLE INFO

#### Article history:

Received 9 June 2013

Revised 16 August 2013

Accepted 19 August 2013

Available online 27 August 2013

#### Keywords:

Glutamate

Cystine

Transporter

Isoxazole

Microwave

### ABSTRACT

Microwave accelerated reaction system (MARS) technology provided a good method to obtain selective and open isoxazole ligands that bind to and inhibit the  $\text{Sx}_{\text{c}-}$  antiporter. The MARS provided numerous advantages, including: shorter time, better yield and higher purity of the product. Of the newly synthesized series of isoxazoles the salicyl hydrazide **6** exhibited the highest level of inhibitory activity in the transport assay. A homology model has been developed to summarize the SAR results to date, and provide a working hypothesis for future studies.

© 2013 Elsevier Ltd. All rights reserved.

System  $\text{Sx}_{\text{c}-}$  ( $\text{Sx}_{\text{c}-}$ ) is an amino acid antiporter that mediates the exchange of extracellular  $\text{l}$ -cystine ( $\text{l}$ -Cys<sub>2</sub>) and intracellular  $\text{l}$ -glutamate ( $\text{l}$ -Glu) across the cellular plasma membrane.<sup>1–4</sup> Initial characterizations of this transporter often focused on the influx of  $\text{l}$ -Cys<sub>2</sub>, as in many cells this uptake serves as a rate-limiting step in providing the intracellular  $\text{l}$ -cysteine ( $\text{l}$ -CysH) required for the synthesis of the antioxidant glutathione (GSH). Within the context of the CNS, however, recent attention has shifted to the 'export side' of the exchange, as the efflux of  $\text{l}$ -Glu through  $\text{Sx}_{\text{c}-}$  carries with it the potential to contribute to excitatory signaling and/or excitotoxic pathology.<sup>1</sup>

Ligands which bind to  $\text{Sx}_{\text{c}-}$  fall into three general categories to date (Chart 1): (i) acyclic amino acids including the endogenous substrates (e.g.,  $\text{l}$ -Glu and  $\text{l}$ -Cys<sub>2</sub>), (ii) isoxazoles and related heterocycles (ibotenic acid (IBO), quisqualic acid (QA), *S*-3-[5-(1-naphthylethyl)-3-carboxy]-isoxazol-4-yl-2-aminopropanoic acid (NACPA), and 4-{1-[2,4-dinitro-phenyl]-hydrazono}-ethyl)-5-(2-naphthalen-2-yl-ethyl)-isoxazole-3-carboxylic acid (NEIH),<sup>5</sup> and (iii) benzoic and sulfonic acids (4-S-carboxy-phenylglycine (CPG), sulfasalazine (SSZ), and *R/S*-4-[4'-carboxyphenyl]-phenylglycine (CBPG)).<sup>6</sup> Recently, Tsukamoto and co-workers explored the structure-activity relationship (SAR) of sulfasalazine and susalimod (SM)<sup>7</sup> analogs determined that the carboxylic acid is essential and that the diazo linker can be replaced with an alkyne, but that

reduction to the alkene or alkyl tether lowered or abolished activity. Studies aimed at the development of <sup>18</sup>F-propyl- $\text{l}$ -glutamate as an  $\text{Sx}_{\text{c}-}$  PET imaging agent demonstrated that the *S,S*-isomer had superior binding affinity to the *R,S*-<sup>8</sup> consistent with earlier observations that the transporter exhibits stereoselectivity of action.<sup>3</sup>

Previously, we reported that the synthesis of hydrazone isoxazole analogs of ACPA (amino-3-carboxy-5-methylisoxazole propionic acid) had promising  $\text{Sx}_{\text{c}-}$  activity.<sup>5</sup> The development of a complete SAR series was, however, limited in that the synthesis was plagued by a ring closure from the isoxazolo[3,4-*d*]pyridazines that resulted in markedly lower biological activities. This was particularly the case when electron donating groups were present on the aryl ring. A mechanistic hypothesis is advanced in which a carbonyl is inserted into the structure to slow or prevent cyclization to the less active [3,4-*d*] by-products. The question to be addressed in this study is whether this structural change will: (1) allow for efficient synthesis and (2) retain bioactivity. This study also presents a comparison between two synthetic methods to prepare the target hydrazones: conventional thermal reflux versus microwave accelerated synthesis, with the goal of shortened reaction time and improved yield.

Isoxazolo[3,4-*d*] pyridazines,<sup>9</sup> exemplified in the first practical synthesis reported by Renzi and Dal Piaz, have been found to both possess interesting biological activities<sup>10</sup> and serve as useful and versatile precursors in medicinal chemistry syntheses.<sup>11</sup> For  $\text{Sx}_{\text{c}-}$  activity, however, the [3,4-*d*] analogs were in all instances found to be less active, indicating that for  $\text{Sx}_{\text{c}-}$  ligand development

\* Corresponding author. Tel.: +1 406 243 4132; fax: +1 406 243 5288.

E-mail address: nicholas.natale@umontana.edu (N.R. Natale).

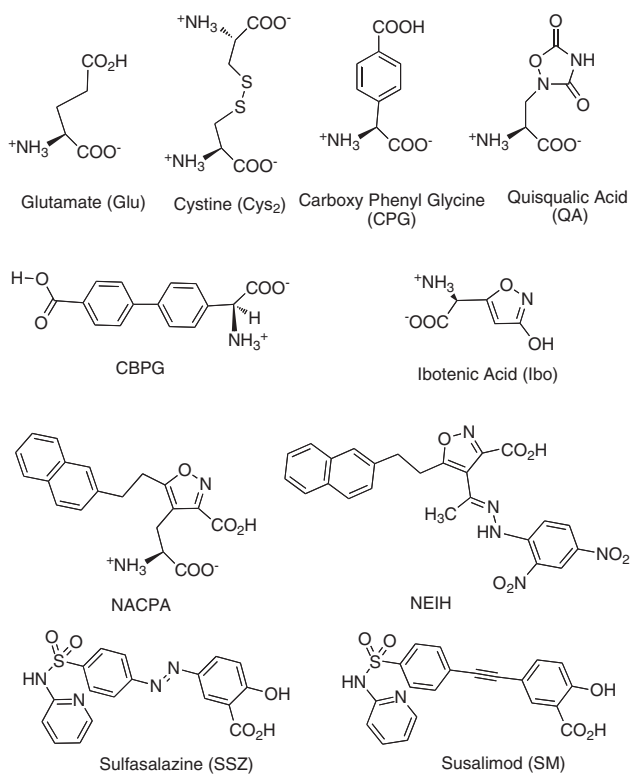


**Chart 1.** Ligand structure training set which bind the system XC-transporter.

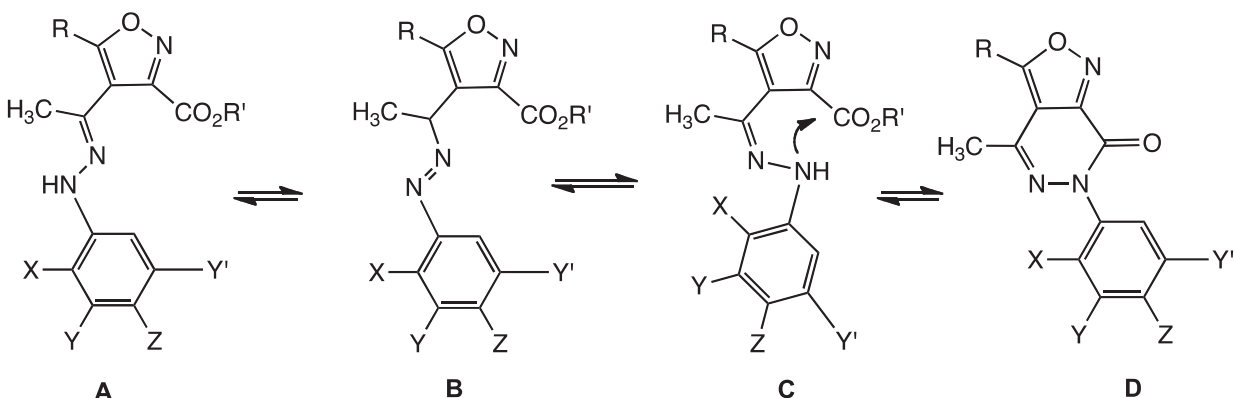
ring closure is undesirable.<sup>5</sup> This ring closure likely occurs via hydrazone to diazene tautomerism as illustrated in **Scheme 1**.<sup>12</sup> Hydrazones of 3-carboethoxy-4-acetyl-isoxazole had previously been prepared without observation of ring closure, and crystallographic characterization showed that they adopted the E-double bond geometry at the C=N of the hydrazone.<sup>13</sup> Reaction to the isoxazolo[3,4-*d*]pyridazinone requires the Z-geometry, which can most reasonably be attained via the intermediacy of the diazene tautomer. A Z-tautomer had been isolated and crystallized in our Sx<sub>c-</sub> study that adopted a conformation in the solid state suggestive of a favorable transition state for ring closure.<sup>5</sup>

The microwave method<sup>14</sup> gave substantially better yields, was largely free of isoxazolo[3,4-*d*]pyridazinone by-product,<sup>14</sup> and exhibited shorter reaction times compared to conventional heating (see **Table 1**).

Within this series, ethyl 4-((*E*)-1-(2-hydroxybenzoyl-hydrozonatoethyl)-5-methylisoxazole-3-carboxylic acid (**6**) exhibited the

highest level of inhibitory activity at Sx<sub>c-</sub> (**Table 1**), comparable to that observed with NEIH.<sup>5</sup> Comparison with (**2**) suggests the presence of an aryl hydroxyl group capable of participating in hydrogen bonding may be advantageous for binding. A moderate level of inhibitory activity was also demonstrated by ethyl 4-((*E*)-1-(1-naphthylbenzoyl-hydrozonatoethyl)-5-methylisoxazole-3-carboxylate (**4**), which supports the hypothesis that having larger aromatic groups enhances binding to the transporter. The insertion of the additional carbonyl in (**1**) and (**2**) resulted in a marked loss of potency compared to the corresponding hydrazones,<sup>5</sup> suggesting that the relative positioning of the aryl groups and the isoxazole ring, as well as the number of electron withdrawing groups, influence the ability of the ligands to interact with lipophilic domains adjacent to the substrate binding site on Sx<sub>c-</sub>.

As a member of the heteromeric amino acid transporter (HAT) family, Sx<sub>c-</sub> is a heterodimer composed of ‘heavy chain’ 4F2hc ( $\approx 80$  kDa) and ‘light chain’ xCT ( $\approx 40$  kDa). The 4F2hc subunit is responsible for trafficking the heterodimer to the plasma membrane, while xCT is responsible for its transport activity. A homology model of Sx<sub>c-</sub> was created based upon the structure of the related ApcT transporter from the thermophile *Methanocaldococcus jannaschii* as crystallized by Gouaux.<sup>15</sup> Thus, the human xCT and ApcT sequences were aligned using ClustalW<sup>18</sup> and threaded over the ApcT crystal structure in its inward-facing apo-form (no substrate bound) (RCSB: pdb 3GIA) using MODELLER.<sup>16,17</sup> Docking studies were carried out using the GOLD docking suite and standard settings.<sup>19</sup> Mutagenesis and thiol-modification experiments on xCT,<sup>28</sup> as well as its analogous position within the water-filled substrate cavity on the ApcT crystal structure<sup>15</sup> suggested that xCT residue Cys327 is in close proximity to the substrate binding site. Docking studies thus examined an 8 Å area surrounding Cys327, which was present at the apex of an obvious cavity in the Sx<sub>c-</sub> homology thread. The resulting models revealed a potential interaction between L-Glu and xCT Arg135, which is located near the central portion of the inward-facing binding pocket. Such an interaction is also consistent with comparative analysis of related transporters that led to the prediction that this residue participates in an H-bond with the distal carboxylate of the bound substrate.<sup>15</sup> Inspection of our model (see *Supplemental material Fig. 1*) also suggested that Tyr244 was participating in the binding, possibly via a π-cation interaction with amino groups. Accordingly, xCT Tyr244 precisely aligned with Tyr202, a residue on a related antiporter (AdiC) shown to participate in binding its substrate L-arginine.<sup>20</sup> Other potential interactions include the α-amino acid head-group of L-Glu and Cys<sub>2</sub> with Tyr244 and the distal γ carboxy (or second α-amino acid head-group) of L-Glu (or L-Cys<sub>2</sub>), with Thr56, Arg135, and Ser330. The analogous roles in the newly identified hydrazide inhibitor **6** are played by the isoxazole-3-carboxyl-



**Scheme 1.** E- to Z-conversion of **A** likely occurs via tautomerization to diazene **B**, and the **Z-C** can cyclize to the isoxazolo[3,4-*d*]pyridazinone **D**.

**Table 1**Microwave versus conventional heating, and inhibition of radiolabeled glutamate uptake by the system  $x_c^-$  transporter

Compound number	Structure	MARS-X, time	Yield %	Conventional reflux, time	Yield %	Hydrolysis %	$[^3\text{H}]$ Glu uptake % of control $\pm$ SD ( $n$ ) <sup>c</sup>
1		15 h	57	1 week	13	28	90 ± 12 (5)
2		75 min	38	48 h	10	34	83 ± 5 (3)
3		10 h	46	1 week	11	29	68 ± 8 (4)
4		50 min	49	1 week	44	21	68 ± 6 (3)
5		110 min	63	1 week	11	80	58 ± 9 (4)
6		80 min	55	40 h	33	41	52 ± 9 (4)

<sup>a</sup> The reaction was conducted in anoxic conditions.<sup>b</sup> Yields are reported after purification by chromatography. Characterization data for the new compounds are given in References <sup>21–26</sup>.<sup>c</sup> SNB-19 cells were assayed for L-[<sup>3</sup>H]-Glu (100  $\mu$ M) uptake under Cl-dependent (Na-free) conditions in the presence of isoxazole-hydrazide derivatives (500  $\mu$ M). Values are reported as mean  $\pm$  SEM ( $n \geq 3$ ) of control activity (accumulation in the absence of inhibitors, i.e., 100%).

ate as depicted in Figure 1A below. The position of the hydroxyphenyl group provides the first insight into the potential location of the lipophilic pocket predicted from earlier SAR studies.<sup>1</sup> The region occupied by **6** also overlaps with other identified inhibitors (Chart 1), particularly the salicylate moieties of SSZ and SM, as well as the distal carboxyphenyl group of CBPG. Interestingly, the gauche sulfonamide of SSZ and SM occupy an analogous orientation to the naphthyl moiety of NACPA, in a lipophilic pocket lined by Phe394 and Trp397. Additional views are illustrated in the Supplementary material.

The ligand–protein close contact interactions suggested from the computational homology models illustrated in Figure 1B and summarized schematically in Figure 1C represents our current working hypothesis. The optimal binding of **6** appears to arise from four principal interactions: (i) a hydrogen bond of Thr56 (TMD1A) with the C3 carboxylate of the isoxazole, (ii) an apparent  $\pi$ -stacking interaction between Arg135 (TMD3) and the isoxazole ring, (iii) a series of lipophilic interactions including Ile142, Tyr244 and Ile134, and (iv) unique to the current new series—a hydrogen bond between Ser330 (TMD8) and the 2-hydroxysalicylylhydrazide moiety. The isoxazolyl hydrazide **6** gave a calculated Goldscore comparable to SM, and higher than all of the other ligands in the training set, including the endogenous substrates. However, these scores, as well as the docking models, must be tempered by the fact that transporters adopts numerous conformations during the transport cycle, of which only one, the occluded inward-facing apo-form of xCT, is examined in the present study.<sup>15,20</sup> While this occluded symmetrical intermediate might be appropriate for modeling fully

bound ligands, the compounds would first have to interact with an outward-facing conformer. Indeed, the ability (or inability) of ligands to bind to different conformers and proceed through the translocation cycle could readily account for difference between computationally-based binding models and assay-based binding data.

As a working hypothesis the homology model suggests several structural features as attractive avenues for further SAR development and biochemical characterization, especially as regards the putative lipophilic pockets. We have recently developed the required synthetic methodology to address this point<sup>27</sup> and will report on our progress in due course.

## Acknowledgments

This work was supported in part by NIH NINDS Grants R21NS067466 (R.B. and N.N.) and P30-NS055022 (J.M. and N.N.). Modeling was carried out in the COBRE supported Molecular Computational Core facility with support from P20RR015583 and NIGMSP20GM103546 (M.B.). L.M. thanks Professor Sandy Ross of the University of Montana Graduate School for a graduate teaching assistantship. J.R. and S.A.S. acknowledge the support of the Neuroscience NSF REU at the University of Idaho.

## Supplementary data

Supplementary data associated with this article can be found, in the online version, at <http://dx.doi.org/10.1016/j.bmcl.2013.08.080>.

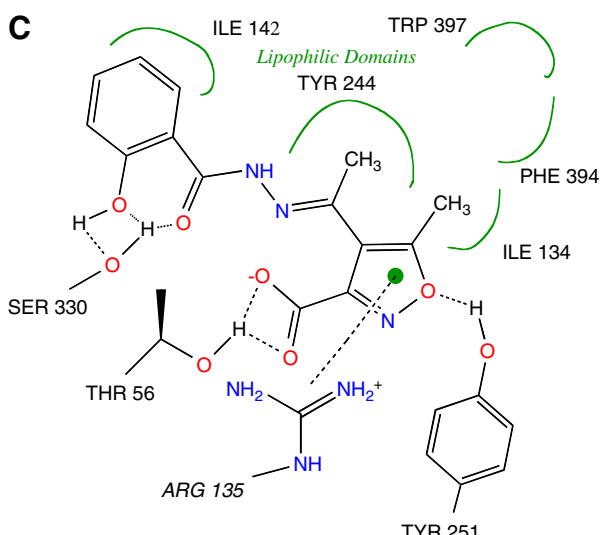
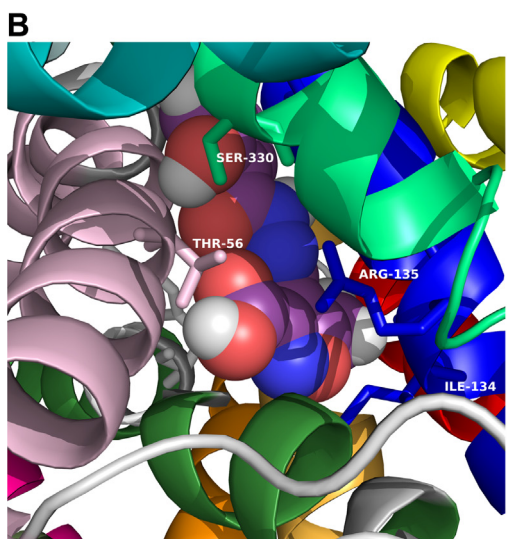
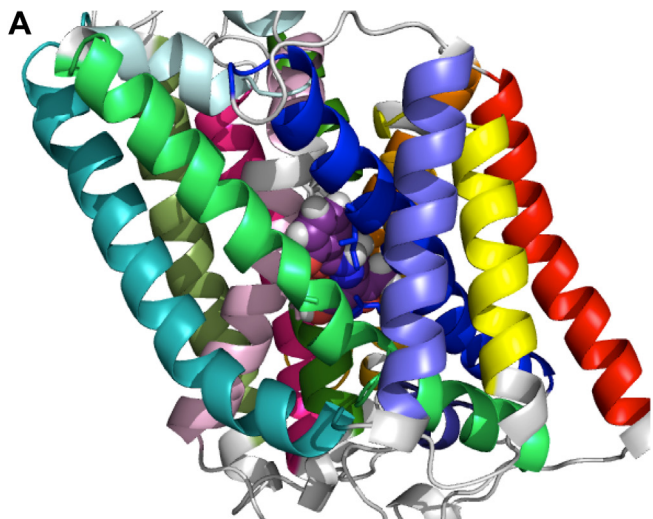


**Figure 1.** (A) Isoxazole hydrazide **6** (space filling, purple) docked in homology model of  $Sx_c$ . (B) Close up view of hydrazide **6** docked in homology model of  $Sx_c$ , showing the key interactions with Ser330, Thr56 and Arg135. (C) Summary of close contacts for **6**.

## References and notes

- (a) Bridges, R. J.; Natale, N. R.; Patel, S. *Br. J. Pharm.* **2012**, *165*, 20; (b) Bridges, R. J.; Lotgen, V.; Lobner, D.; Baker, D. A. *Pharmacol. Rev.* **2012**, *64*, 780.
- Glutamate and GABA Receptors and Transporters, Structure Function and Pharmacology*; Egebjerg, J., Schousboe, A., Krosgaard-Larsen, P., Eds.; Taylor and Francis: New York, 2002.
- Bridges, R. J.; Patel, S. A. In *Topics in Medicinal Chemistry*; Napier, S., Ed.; Springer: New York, 2009; pp 187–222, Vol. 4.
- Natale, N. R.; Magnusson, K.; Nelson, J. K. *Curr. Top. Med. Chem.* **2006**, *6*, 823.
- Patel, S. A.; Rajale, T.; O'Brien, E.; Burkhardt, D. J.; Nelson, J. K.; Twamley, B.; Blumenfeld, A.; Szabon-Watola, M. I.; Gerdes, J. M.; Bridges, R. J.; Natale, N. R. *Bioorg. Med. Chem.* **2010**, *18*, 202.
- Etoga, J. L.; Ahmed, S. K.; Patel, S.; Bridges, R. J.; Thompson, C. M. *Bioorg. Med. Chem.* **2010**, *20*, 2680.
- Shukla, K.; Thomas, A. G.; Ferraris, D. V.; Hin, N.; Sattler, R.; Alt, J.; Rojas, C.; Slusher, B. S.; Tsukamoto, T. *Bioorg. Med. Chem. Lett.* **2011**, *21*, 6184.
- Koglin, N.; Mueller, A.; Berndt, M.; Schmitt-Willrich, H.; Toschi, L.; Stephens, A. W.; Gekeler, V.; Friebel, M.; Dinkelborg, L. M. *Clin. Cancer Res.* **2011**, *17*, 6000.
- (a) Renzi, G.; Dal Piaz, V. *Gazz. Chim. Ital.* **1965**, *95*, 1478–1491; (b) Renzi, G.; Pinzauti, S. *Il Farmaco Ed. Sci.* **1969**, *24*, 885; (d) Dal Piaz, V.; Pinzauti, S.; Lacrimini, P. *J. Heterocycl. Chem.* **1975**, *13*, 409; (d) Chimichi, S.; Ciciani, G.; Dal Piaz, V.; De Sio, F.; Sarti-Fantoni, P.; Torroba, T. *Heterocycles* **1986**, *24*, 3467; (e) Dal Piaz, V.; Graziano, A.; Haider, N.; Holzer, W. *Magn. Reson. Chem.* **2005**, *43*, 240.
- Montesano, F.; Barlocco, D.; Dal Piaz, V.; Leonardi, A.; Poggesi, E.; Fanelli, F.; De Benedetti, P. G. *Bioorg. Med. Chem.* **1998**, *6*, 925; Costantino, L.; Rastelli, G.; Gamberini, M. C.; Giovannoni, M. P.; Dal Piaz, V.; Vianello, P.; Barlocco, D. *J. Med. Chem.* **1999**, *42*, 1894; (c) Dal Piaz, V.; Rascon, A.; Dubra, M.; Giovannoni, M. P.; Vergelli, C.; Castellana, M. C. *Il Farmaco* **2002**, *57*, 89.
- (a) Dal Piaz, V.; Ciciani, G.; Chimichi, S. *Heterocycles* **1985**, *23*, 365; (b) Dal Piaz, V.; Ciciani, G.; Turco, G.; Giovannoni, M. P.; Miceli, M.; Pirisino, R.; Perretti, M. J. *J. Pharm. Sci.* **1991**, *80*, 1417; (c) Dal Piaz, V.; Giovannoni, M. P.; Ciciani, G.; Barlocco, D.; Giardina, G.; Petrone, G.; Clarke, G. D. *Eur. J. Med. Chem.* **1996**, *31*, 65; (d) Dal Piaz, V.; Giovannoni, M. P.; Castellana, M. C.; Palacios, J. M.; Beleta, J.; Domenech, T.; Segarra, V. *J. Med. Chem.* **1997**, *40*, 1417; (e) Barlocco, D.; Cignarella, G.; Dal Piaz, V.; Giovannoni, M. P.; De Benedetti, P. G.; Fanelli, F.; Montesano, F.; Poggesi, E.; Leonardi, A. *J. Med. Chem.* **2001**, *44*, 2403; (f) Paola, M.; Giovannoni, M. P.; Dal Piaz, V.; Kwon, B.-M.; Kim, M.-K.; Toma, L.; Barlocco, D.; Bernini, F.; Canavesi, M. J. *Med. Chem.* **2001**, *44*, 4292; (g) Giovannoni, M. P.; Cesari, N.; Vergelli, C.; Graziano, A.; Biancalani, C.; Biagini, P.; Ghelardini, C.; Vivoli, E.; Dal Piaz, V. *J. Med. Chem.* **2007**, *50*, 3945; (h) Biancalani, C.; Giovannoni, M. P.; Pieretti, S.; Cesari, N.; Graziano, A.; Vergelli, C.; Cilibazzi, A.; Di Gianuario, A.; Colucci, M.; Mangano, G.; Garrone, B.; Polenzani, L.; Dal Piaz, V. *J. Med. Chem.* **2009**, *52*, 7397.
- (a) Ozen, A. S.; Doruker, P.; Aviyente, V. *J. Phys. Chem. A* **2007**, *111*, 13506; (b) Ramanathan, S.; Lemal, D. M. *J. Org. Chem.* **2007**, *72*, 1566; (c) Fattorusso, C.; Campiani, G.; Kukreja, G.; Persico, M.; Butini, S.; Romano, M. P.; Attarelli, M.; Ros, S.; Brindisi, M.; Savini, L.; Novellino, E.; Nacci, V.; Fattorusso, E.; Parapini, S.; Basilico, N.; Taramelli, D.; Yardley, V.; Croft, S.; Borriello, M.; Gemma, S. *J. Med. Chem.* **2008**, *51*, 1333; (d) Blanco, F.; Egan, B.; Caboni, L.; Elguero, J.; O'Brien, J.; McCabe, T.; Fayne, D.; Meegan, M. J.; Lloyd, D. G. *J. Chem. Inf. Model.* **2012**, *52*, 2387.
- (a) Burkhardt, D. J.; Vij, A.; Natale, N. R. *J. Chem. Crystallogr.* **1999**, *29*, 749; (b) Natale, N. R.; Szabon-Watola, M. I.; Twamley, B.; Bridges, R. J.; Patel, S.; Rajale, T. *Acta Crystallogr.* **2009**, *E65*, o144.
- (a) Andrade, M. M.; Barros, M. T. *J. Comb. Chem.* **2010**, *12*, 245; (b) La Regina, G.; Gatti, V.; Piscitelli, F.; Silvestri, R. *ACS Comb. Sci.* **2011**, *13*, 2.
- Shaffer, P. L.; Goehring, A.; Shankaranarayanan, A.; Gouaux, E. *Science* **2009**, *325*, 1010.
- Pearson, W. R.; Lipman, D. J. *Proc. Natl. Acad. Sci. U.S.A.* **1988**, *85*, 2444.
- Sali, A.; Blundell, T. L. *J. Mol. Biol.* **1993**, *234*, 779.
- Larkin, M. A.; Blackshields, G.; Brown, N. P.; Chenna, R.; McGettigan, P. A.; McWilliam, H.; Valentin, F.; Wallace, I. M.; Wilm, A.; Lopez, R.; Thompson, J. D.; Gibson, T. J.; Higgins, D. G. *Bioinformatics* **2007**, *23*, 2947.
- Verdonk, M. L.; Cole, J. C.; Hartshorn, M. J.; Murray, C. W.; Taylor, R. D. *Proteins* **2003**, *52*, 609.
- Kowalczyk, L.; Ratera, M.; Paladino, A.; Bartoccioni, P.; Errasti-Murugarren, E.; Valencia, E.; Portella, G.; Bial, S.; Zorzano, A.; Fita, I.; Orozco, M.; Carpena, X.; Vázquez-Ibarra, J. L.; Palacín, M. *Proc. Natl. Acad. Sci. U.S.A.* **2011**, *108*, 3935.
- Analytical data for new compounds: 4-(*E*)-1-(3,5-bis(trifluoromethyl)benzoylhydrazone)ethyl)-5-methylisoxazole-3-carboxylic acid, **1**.  $^1\text{H}$  NMR (500 MHz, CDCl<sub>3</sub>): δ 8.49 (s, 1H), 8.42 (s, 1H), 8.29 (b s, 2H), 8.04 (s, 1H), 7.93 (m, 1H), 7.76 (s, 1H), 2.86 (s, 3H), 2.50 (s, 3H);  $^{13}\text{C}$  NMR (125 MHz, CDCl<sub>3</sub>) δ 170.6, 167.2, 164.7, 154.9, 151.5, 141.6, 132.6, 132.3, 132.1, 132.0, 130.1, 127.8, 122.7 (q, *J* = 272 Hz), 112.6, 29.7, 19.2; IR cm<sup>-1</sup>; ESI-MS for C<sub>16</sub>H<sub>11</sub>F<sub>6</sub>N<sub>3</sub>O<sub>4</sub>+H m/z 423.9705 (100%).
- 4-(*E*)-1-(Benzoylhydrazone)ethyl)-5-methylisoxazole-3-carboxylic acid, **2**. Mp 152–154 °C.  $^1\text{H}$  NMR (500 MHz, CDCl<sub>3</sub>): δ 11.90 (s, 1H), 8.08 (d, *J* = 8.40 Hz, 1H), 7.89 (d, *J* = 5.50 Hz, 1H), 7.81 (m, 1H), 7.68 (m, 1H), 7.61 (t, *J* = 7.70 Hz, 1H), 7.52 (m, 1H), 7.46 (m, 1H),  $^{13}\text{C}$  NMR 177.5, 170.4, 169.2, 159.9, 158.6, 154.3, 128.9, 116.4, 109.9, 49.8; IR cm<sup>-1</sup>; 2305, 2926, 2850, 2625, 2107, 1688, 1624, 1580, 1447, 1376, 1187; ESI-MS for C<sub>14</sub>H<sub>13</sub>N<sub>3</sub>O<sub>4</sub>+H m/z 288.0794 [100%].
- 4-(*E*)-1-(4-Methoxybenzoylhydrazone)ethyl)-5-methylisoxazole-3-carboxylate, **3**.  $^1\text{H}$  NMR (500 MHz, CDCl<sub>3</sub>): δ 7.82 (d, *J* = 7.5 Hz, 1H), 6.94 (d, *J* = 7.5 Hz, 1H),

- 4.41 ( $q, J = 4.5$  Hz, 2H), 3.85 (s, 3H), 2.44 (s, 3H), 2.23 (s, 3H), 1.39 (t,  $J = 7.5$  Hz, 3H);  $^{13}\text{C}$  NMR (125 MHz,  $\text{CDCl}_3$ ):  $\delta$  169.1, 162.6, 158.9, 129.1, 124.7, 113.9, 62.3, 55.44, 16.9, 13.9, 11.8; ESI-MS for  $\text{C}_{15}\text{H}_{15}\text{N}_3\text{O}_5+\text{H}$   $m/z$  318.1046 (100%).
24. *Ethyl 4-((E)-1-Naphthoylhydrazono)ethyl)-5-methylisoxazole-3-carboxylic acid, 4.* Mp 146–148 °C.  $^1\text{H}$  NMR (500 MHz, methanol- $d_4$ ):  $\delta$  12.80 (s, 1H), 8.95 (d,  $J = 8.50$  Hz, 1H), 8.52–8.31 (m, 1H), 8.08–7.88 (m, 2H), 7.68–7.47 (m, 3H), 3.62 (s, 1H), 2.87 (s, 3H), 2.42 (s, 3H);  $^{13}\text{C}$  NMR (125 MHz, methanol- $d_4$ )  $\delta$  191.1, 171.9, 171.8, 164.9, 160.7, 151.9, 149.1, 134.0, 131.6, 130.8, 129.9, 129.0, 127.7, 127.1, 126.8, 125.6, 125.5, 124.4, 124.1, 19.3, 19.1, 13.9, 13.7; IR  $\text{cm}^{-1}$  3310, 3199, 2985, 2190, 1736, 1644, 1519, 1458, 1373, 1356, 1278, 1260, 1044; ESI-MS for  $\text{C}_{18}\text{H}_{15}\text{N}_3\text{O}_5+\text{H}$   $m/z$  338.0835 [100%].
25. *Ethyl 4-((E)-1-(2,4-difluorobenzoylhydrazono)ethyl)-5-methylisoxazole-3-carboxylic acid, 5.*  $^1\text{H}$  NMR (500 MHz,  $\text{CDCl}_3$ ):  $\delta$  8.26 (d,  $J = 6.5$  Hz, 1H), 7.60 (s, 1H), 7.03 (d,  $J = 9.5$  Hz, 1H), 2.66 (s, 3H), 2.39 (s, 3H);  $^{13}\text{C}$  NMR (125 MHz,  $\text{CDCl}_3$ ):  $\delta$  171.9, 166.2, 164.8, 159.9, 134.5, 116.5, 112.8, 112.6, 18.4, 13.2; IR 2923.64, 2227.91, 1662.72, 1611.32, 1497.22  $\text{cm}^{-1}$ ; ESI-MS for  $\text{C}_{14}\text{H}_{11}\text{F}_2\text{N}_3\text{O}_4+\text{H}$   $m/z$  323.9794 [100%].
26. *Ethyl 4-((E)-1-(2-hydroxybenzoylhydrozono)ethyl)-5-methylisoxazole-3-carboxylic acid, 6.*  $^1\text{H}$  NMR (500 MHz,  $\text{CDCl}_3$ ):  $\delta$  9.17 (s, 1H), 7.91 (d, 1H), 7.42 (m, 2H), 7.00 (m, 1H), 6.82 (m, 1H), 5.37 (s, 1H); 3.6 (s, 3H), 2.41 (s, 3H);  $^{13}\text{C}$  NMR (125 MHz,  $\text{CDCl}_3$ )  $\delta$  197.0, 167.8, 166.6, 161.8, 135.3, 133.8, 129.8, 128.9, 126.9, 118.3, 116.6, 113.6, 21.7, 13.1; IR  $\text{cm}^{-1}$  3206, 3068, 2924, 2853, 2228, 1658, 1619, 1457, 1381, 1318, 1276, 1259, 1173, 1093. ESI-MS for  $\text{C}_{14}\text{H}_{13}\text{N}_3\text{O}_5+\text{H}$   $m/z$  304.1637 [100%].
27. (a) McDaniel, S. W.; Keyari, C. M.; Rider, K. C.; Natale, N. R.; Diaz, P. *Tetrahedron Lett.* **2011**, *52*, 5656; (b) Rider, K. C.; Burkhardt, D. J.; Li, C.; McKenzie, A. R.; Nelson, J. K.; Natale, N. R. *ARKIVOC* **2010**, *97*. Part (viii).
28. Gasol, E.; Jimenez-Vidal, M.; Chillaron, J.; Zorzano, A.; Palacin, M. *J. Biol. Chem.* **2004**, *279*, 31228.